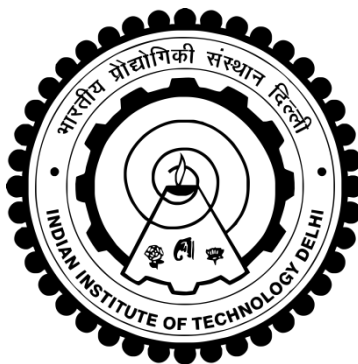


**FOAMABILITY OF POLYPROPYLENE AND ITS BLENDS
WITH ETHYLENE ACRYLIC ELASTOMER MODIFIED
BY GAMMA RADIATION**

ANINDYA DUTTA



DEPARTMENT OF MATERIALS SCIENCE AND ENGINEERING

INDIAN INSTITUTE OF TECHNOLOGY DELHI

MAY 2019

© Indian Institute of Technology Delhi (IITD), New Delhi, 2019

**FOAMABILITY OF POLYPROPYLENE AND ITS
BLENDS WITH ETHYLENE ACRYLIC ELASTOMER
MODIFIED BY GAMMA RADIATION**

by

ANINDYA DUTTA

Department of Materials Science and Engineering

Submitted

in fulfillment of the requirements of the degree of Doctor of Philosophy

to the



INDIAN INSTITUTE OF TECHNOLOGY DELHI

MAY 2019

“If an egg is broken by an outside force, life ends.

If broken by an inside force, life begins.

Great things always begin from the inside”

– Jim Kwik.

Dedicated

To My

Mother “Late Reba Dutta”

&

Wife “Saheli Bhattacharyya”

CERTIFICATE

*This is to certify that the thesis entitled, “Foamability of Polypropylene and Its Blends with Ethylene Acrylic Elastomer Modified by Gamma Radiation” submitted by Mr. Anindya Dutta to the Indian Institute of Technology Delhi, for the fulfillment of award of the degree, **Doctor of Philosophy**, is a record of bonafide research work carried out by him under my supervision and guidance. This thesis has been prepared in conformity with the rules and regulations of the Indian Institute of Technology Delhi, New Delhi.*

*The thesis, in my opinion, is worthy of consideration for award of the degree of **Doctor of Philosophy** in accordance with the regulations of the Institute. To the best of my knowledge, the results embodied in the thesis have not been submitted to any other University or Institute for the award of any other Degree or Diploma.*

(Anup K. Ghosh)

Professor and HOD

Department of Materials Science and Engineering

Date -

Indian Institute of Technology Delhi

Place – New Delhi

Hauz Khas, New Delhi – 110016, India

Acknowledgements

It gives me immense pleasure to express my deep sense of gratitude to all who have helped me along my way through the doctoral studies and a memorable stay at IIT Delhi.

I express my profound sense of gratitude and veneration to my supervisor, Prof. Anup K. Ghosh for guiding me all the way during my PhD tenure. I have gained a lot by his able guidance, practical experience, patience and detailed corrections of all my reports. His constant inspiration and encouragement have been a great motivation for me behind all the work I have conducted. I appreciate his way of informal teaching on handling things with patience and maturity, writing of manuscripts or reports for different audiences or platforms and these helped me to tide over the difficult situations. Many a times his pretension of being hard helped me to be stronger towards the failures and motivated me to work harder. He has always boosted me to put in extra efforts and I am indebted to them what I am today. I am also thankful to him for providing me opportunities to handle some short-term projects and assisting them in few industrial projects which enabled me to fortify my skills.

I express my deep sense of gratitude to my student research committee members, Prof. S. N. Maiti, Prof. Bhabani K. Satapathy, and Prof. Naresh Bhatnagar who have monitored my work and provided me the valuable suggestions. I am also thankful to Prof. Veena Choudhary, Prof. Josemon Jacob, Prof. Rajesh Prasad, Dr. Nitya Nand Gosvami, Dr. Jayant Jain, Dr. Suresh Neelakantan, Dr. Leena Nebhani, Dr. Sampa Saha and Dr. Bijay P. Tripathi who in spite of their busy schedule have always made themselves available for valuable discussions and support.

I would like to extend my thanks to Dr. D. K. Avasthi, Mr. Debashish Sen and Mr. Birendra Singh, IUCA, New Delhi for their kind support by providing gamma radiation facility to carry out irradiation of samples in his laboratory. I would like to convey my special thanks to Dr. Shashi Motilal for her support and encouragement.

This work would not be possible without the support and encouragement from my friends, seniors and juniors. My special thanks go to Dr. Manash Jyoti Kashyap, Dr. Satish Kommoji, Dr. Sneh Bharti, Dr. Shikha Jain, Dr. Jutika Goswami, Dr. Priyanka Singh, Dr. Rishi Sharma, Dr. Sunil Kumar, Dr. Rajender Malik Dr. Pawan Verma, Dr. Rakesh Kumar Kachhap,

Dr. Abhishek Gandhi, Dr. Md. Tahir Zafar, Dr. Sabapathy Sankarpandi, Ms. Swarna, Dr. Ritima Banerjee, Miss. Prajesh Nayak, Miss. Bariya Qayyum, Miss. Srijita Purkayastha, Dr. Astha Garhwal, Dr. Achala, Dr. Ranjana Nehra, Dr. Rajendra Singla, Dr. Harjeet Singh Jaggi, Dr. Harshita, Miss. Sucharita Sethy, Ms. Savita Meena, Dr. Debang Konwar, Dr. Bhavana Sharma, Miss. Banpreet Kaur, Dr. Meenakshi Verma, Dr. Sampat Singh Chauhan, Dr. V.P. Singh, Mr. Devender Mogha, Ms. Shilpi Sharma, Dr. Pragati Ghalout, Miss. Sumbul Hafeez, Miss. Ifra, Mr. Agni Kumar Biswal, Miss. Smrutirekha Mishra, Miss. Shubhra Goel, Miss. Deepika Sharma, Miss. Sikha, Mr. Ashok Bakshi, Miss. Kalpana Pandey, Miss. Tina Joshi, Miss. Shaifali Dhingra, Miss. Aanchal Jaisingh, Miss. Shivani Goyal, Miss. Swati Mishra, Mr. Debarghya Saha, Mr. Ehteshamul Islam, Mr. Anubhav Kumar, Miss. Kanupriya Nayak, Mr. Saroj Kumar Samantray, Miss. Huma Khan, Mr. Ajit Babarao Bhagat, Mr. Gaurav, Mr. Shanta Mohapatra, Mr. Aditya Gokhale, Mr. Hemant K. Sharma, Mr. Anand Verma, Ms. Aravi Muzaffar, Mr. Prashant Mittal, Mr. Vicky Nandal, Mr. Deepak Kumar, Mr. Shrikanth S., Mr. Ranjeet Kumar, Mr. Nooruddin Ansari, Mr. Amit Kumar Prasad, Mr. Kasimuthuma Niyans, Mr. Abhishek Rastogi, Ms. Supriya Maity, Mr. Biswajit Mishra, Ms. Pooja Vardhini Natesan, Mr. Harshal Vinod Peshne, Mr. Mayank Prakash, Mr. Likkumanul Hakkim N., Ms. Aiswarya T. T., Mr. Ujjawal Bairagi, Mr. Abhishek Rastogi, Mr. Chetan Singh, Mr. Jayant Kadu, Miss. Anasuya Roy Chowdhury, Mr. Debjyoti Banerjee and Mr. Arnav Ghosh for their cooperation and friendly attitude. I would like to convey my special thanks to Dr. Sabapathy Sankarpandi, Ms. Swarna for providing me motivational and moral support from time to time in my research carrier. I would also like to convey my special gratitude to my best friends, Dr. Pranab Dey and Dr. Pratap Roy for their enormous encouragement and healthy interactions, happened to be very refreshing time to time.

I owe thanks to laboratory staffs Mr. Ashok Kapoor, Mr. Surender Sharma, Mr. Shiv Kant, Mr. Ehteshamul Islam, Mr. Gajraj Singh, Mr. Vijay Tiwari, Mr. Tulsi Ram Pal, Mr. Jitendra Rathore and Mr. Saroj Kumar for their timely help and suggestions. I would also like to convey my thanks to Mr. Adarsh Sehgal, Mr. Subhas Chand, Mr. Narender Kumar, Ms. Shalini Arora, Ms. Sunita Dang, Mr. Sudhir Kumar Pandey and Mr. Pramod Kale for their all possible supports. I am grateful to Mr. D. C. Sharma, Mr. Kuldeep Sharma, Mr. Mahesh Soni and Ms. Aastha Sharma of SEM central facility for teaching and allowing me the SEM of my samples.

I wish to acknowledge Ministry of Human Resource Development (MHRD), Government of India, for providing me financial assistance to carry out my research work smoothly.

I take this opportunity to express my deepest gratitude to my family members. The love from my father, Mr. Daiba Nidhan Dutta and mother-in-law, Ms. Rita Bhattacharyya has always given me the strength and confidence to overcome the difficulties and to accomplish the objectives in my life. They always stood by my side with their emotional support, and blessings. I also thank my brother Mr. Arpan Datta, sister-in-law Ms. Shnaoli Bhattacharyya and her husband Mr. Koustav Banerjee for their unconditional love and happy moments during all the family gatherings. I am in short of words to acknowledge my strength and stable force, my better half, Ms. Saheli Bhattacharyya. She is most understanding person in my life and I want to express my regard for every moment we lived together, for all the efforts to make me happy and complete. She always stood by my side with a smile during the storms came across in pursuing M.Tech and PhD. It would be very meager attempt, if I say thanks to my caregiver cum homemaker Mr. Tapan Karmakar for his immense effort to bring me up to this stage. Finally and above all, I would like to thank the Almighty God. It would not have been possible for me to reach at this stage of academic pursuit without his grace.



Date:

(Anindya Dutta)

Place: New Delhi.

ABSTRACT

The present study dealt with the introduction of crosslinks in ethylene acrylic elastomer and further checking of foamability of polypropylene (PP)/ γ -irradiated ethylene acrylic (AEM) elastomer blends and finally the mechanical performances of the foams were evaluated. In present study, foaming of blends was done with supercritical CO₂ in a batch mode. Initially, optimization of microcellular foam processing of PP/unirradiated ethylene acrylic elastomer blends was carried out through design of experiment approach using Taguchi technique and the correlation among foamability, morphological and rheological parameters of blends was established. In this section, blends with low elastomer content (10 wt.%) were optimized for better foamability. Furthermore, γ -irradiation was done of PP/unirradiated AEM elastomer blends at several radiation doses not only to optimize the γ -irradiation dose but also to optimize the elastomer concentration of blend in terms of degradability during melt processing of blends. Radiation dose of 25 kGy was determined to be optimum in terms of degradation of PP/unirradiated elastomer blend. After the optimization of elastomer concentration, in order to identify the effect of extent of crosslinking of elastomer and the effect of blend morphology on the foamability of PP/ γ -irradiated elastomer blends, crosslinking of ethylene acrylic elastomer was carried out using γ -radiation with several doses prior to melt blending and subsequently 10 wt.% of the irradiated elastomers (optimized previously) were mixed with PP in a micro-compounder at three different screw speeds to attain distinct morphological differences among blends. The microcellular morphology development of blends with foaming was analyzed with the screw speed, extent of crosslinking and foaming temperature. Preferences of homogenous and heterogeneous cell nucleation were explained through the surface tension and interfacial

energy of neat polymers [in presence of air and liquid e.g. water and poly(ethylene glycol) 200 (PEG200)]. Additionally, the mechanical responses of PP/ γ -irradiated ethylene acrylic elastomer blends were compared with the results of PP/unirradiated ethylene acrylic elastomer blends. Gamma radiation of AEM elastomer was done at 25 kGy optimized irradiation dose. Moreover, thorough correlations was drawn among the mechanical characteristics of blends with their morphological (SEM, WAXD), thermal (DSC), thermo-mechanical (DMA), rheological (frequency sweep) and fractured surface morphological aspects. From several theoretical models, fitted with mechanical parameters of blends, it was determined that the γ -irradiated elastomer had lesser interfacial adhesion with PP than the unirradiated elastomer. Finally, the mechanical performances of foams of PP/ γ -irradiated elastomer blends were evaluated and made a comparative study with the mechanical data of foams of PP/unirradiated elastomer blends. Microcellular foam morphology was observed for blends; whereas, for PP submicron and irregular foam morphology was noticed. The yielding behavior of blends was marginalized and the yielding of blends with γ -irradiated elastomer was decimated. Most interestingly, necking phenomenon and strain induced crystallization could be observed for foams of blends. Tensile modulus of foam sample was significantly increased by 3 times. From the impact fractured surface morphologies of foams, the enhanced impact strength of foams could be perceived.

सार

वर्तमान अध्ययन ने एथिलीन ऐक्रेलिक इलास्टोमेर में क्रॉसलिंग की शुरुआत और पॉलीप्रोपाइलीन (पीपी) / γ -विकिरणित एथिलीन ऐक्रेलिक (ईईएम) इलास्टोमेर मिश्रणों की फोमिंग की जांच की और आखिरकार फोम के यांत्रिक प्रदर्शन का मूल्यांकन किया गया। वर्तमान अध्ययन में, एक बैच मोड में सुपरक्रिटिकल कार्बन डाइऑक्साइड के साथ मिश्रणों की फोमिंग की गई थी। प्रारंभ में, पीपी / अविकिरणित इथाइलीन ऐक्रेलिक इलास्टोमेर मिश्रणों के माइक्रोसेलुलर फोम प्रसंस्करण का अनुकूलन टैगुची तकनीक का उपयोग करते हुए प्रयोग दृष्टिकोण के डिजाइन के माध्यम से किया गया था और मिश्रणों के फोमेबिलिटी, रूपात्मक और रियोलॉजिकल मापदंडों के बीच संबंध स्थापित किया गया था। इस खंड में, कम एलास्टोमेर सामग्री (10 wt%) के साथ मिश्रण बेहतर फोमेबिलिटी के लिए अनुकूलित किया गया था। इसके अलावा, γ -विकिरण पीपी / अविकिरणित ईईएम इलास्टोमेर मिश्रणों पर किया गया था, जो कई विकिरण खुराक पर न केवल विकिरण खुराक को अनुकूलित करने के लिए, बल्कि मिश्रणों के पिघल प्रसंस्करण के दौरान क्षरण की दृष्टि से इलास्टोमेर एकाग्रता का अनुकूलन करने के लिए भी किया गया था। 25 kGy की विकिरण खुराक पीपी / अविकिरणित इलास्टोमेर मिश्रण के क्षरण के संदर्भ में इष्टतम होने के लिए निर्धारित की गई थी। इलास्टोमेर एकाग्रता के अनुकूलन के बाद, इलास्टोमेर के क्रॉसलिंग की सीमा के प्रभाव की पहचान करने और पीपी / γ -विकिरणित इलास्टोमेर मिश्रणों की फेनिलबिलिटी पर मिश्रण आकारिकी के प्रभाव की पहचान करने के लिए, एथिलीन ऐक्रेलिक इलास्टोमेर के क्रॉसलिंग को कई खुराकें γ -विकिरण के साथ उपयोग किया गया मिश्रणों को पिघलाने से पहले, और बाद में 10 wt% विकिरणित इलास्टोमर्स का (पहले से अनुकूलित) मिश्रणों के बीच अलग-अलग रूपात्मक मतभेदों को प्राप्त करने के लिए तीन अलग-अलग पंच गति पर एक माइक्रो-कंपाउंडर में पीपी के साथ मिलाया गया था। फोमिंग के साथ मिश्रणों के सूक्ष्म कोशिकीय विकास का विश्लेषण पंच गति, क्रॉसलिंग की सीमा और झाग तापमान के साथ किया गया था। सजातीय और विषम सेल न्यूक्लियेशन की वरीयताएँ सतह के तनाव और स्वच्छ पोलिमेर की अंतरापणीय ऊर्जा के माध्यम से समझाई गई [वायु और

तरल की उपस्थिति में उदा। पानी और पाली (इथाइलीन ग्लाइकॉल) 200 (PEG200)]। इसके अतिरिक्त, पीपी / γ -विकिरणित एथिलीन ऐक्रेलिक इलास्टोमेर मिश्रणों के यांत्रिक प्रतिक्रियाओं की तुलना पीपी / अविकिरणित एथिलीन ऐक्रेलिक इलास्टोमेर मिश्रणों के परिणामों के साथ की गई थी।

ईईएम इलास्टोमेर का γ -विकिरण 25 kGy अनुकूलित विकिरण खुराक पर किया गया था। इसके अलावा, उनके रूपात्मक (SEM, WAXD), थर्मल (DSC), थर्मो-मैकेनिकल (DMA), रियोलॉजिकल (Frequency sweep) और खंडित सतह आकारिकी पहलुओं के साथ मिश्रणों की यांत्रिक विशेषताओं के बीच पूरी तरह से सहसंबंध तैयार किए गए थे। कई सैद्धांतिक मॉडलों से, मिश्रणों के यांत्रिक मापदंडों से सुसज्जित, यह निर्धारित किया गया था कि γ -विकिरणित इलास्टोमेर में पीपी के साथ अविकिरणित इलास्टोमेर की तुलना में कम इंटरफेशियल आसंजन था। अंत में, पीपी / γ -विकिरणित इलास्टोमेर मिश्रणों के झागों के यांत्रिक प्रदर्शन का मूल्यांकन किया गया और पीपी / अविकिरणित इलास्टोमेर मिश्रणों के यांत्रिक दत्त-सामग्री के साथ एक तुलनात्मक अध्ययन किया गया। मिश्रणों के लिए माइक्रोकेलुलर फोम आकृति विज्ञान देखा गया था; जबकि, पीपी के लिए उप माइक्रोन और अनियमित फोम आकारिकी देखा गया था। मिश्रणों के उपज व्यवहार को हाशिए पर रखा गया था और γ -विकिरणित इलास्टोमेर के साथ मिश्रणों की उपज को हटा दिया गया था। सबसे दिलचस्प बात, नेकिंग की घटना और तनाव प्रेरित क्रिस्टलीकरण मिश्रणों के फोम के लिए मनाया जा सकता है। फोम के नमूने के तन्यता मापांक में 3 गुना की वृद्धि हुई थी। फोम के खंडित सतह आकारिकी के प्रभाव से, फोम की बढ़ी हुई प्रभाव शक्ति को माना जा सकता है।

TABLE OF CONTENTS

Certificate.....	i
Acknowledgement	ii
Abstract.....	v
Table of Contents	vii
List of Figures.....	xv
List of Tables	xxiii
List of Equations	xxv
List of Abbreviations	xxvi
List of Symbols	xxix

Chapter-1: Introduction and literature review

1.1 Preamble	1
1.2 Introduction.....	4
1.2.1 Introduction of foams	4
1.2.2 Types of foam.....	4
1.2.3 Blowing agents	5
1.2.4 Polyolefins and their foaming	7
1.2.5 Steps in foaming processes	8

1.2.6	Foaming methods for thermoplastics using physical blowing agent	9
1.2.6.1	<i>Extrusion foaming</i>	9
1.2.6.2	<i>Microcellular injection moulding</i>	10
1.2.6.3	<i>Batch/Solid state foaming</i>	11
1.2.6.4	<i>Bead foaming</i>	12
1.3	Literature review	13
1.3.1	Gas dissolution in amorphous and crystalline polymers and its effect on foaming	13
1.3.2	Effects of rheological, thermal and morphological attributes on foaming	15
1.3.2.1	<i>Dependency on rheological characteristics</i>	15
1.3.2.2	<i>Dependency on thermal characteristics of polymer</i>	17
1.3.2.3	<i>Dependency on morphological aspects</i>	19
1.3.3	Homogeneous and heterogeneous nucleation in foaming.....	22
1.3.4	Foaming of polypropylene	25
1.3.5	Effect of elastomer addition on polypropylene foaming.....	26
1.3.6	Effect of crosslinking on foaming of polymers and benefits of gamma radiation	28
1.3.7	Ethylene acrylic elastomer (AEM) elastomers, their blends and effect of high energy radiation.....	29
1.3.8	Effect of high energy radiation of polypropylene and its blends	30
1.3.9	Effect of degree of crosslinking on foaming of blends of PP	31
1.4	Literature outcomes & gaps, objective, scope and plan of work	32
1.4.1	Literature outcomes	32
1.4.2	Literature gaps	33
1.4.3	Objective	34
1.4.4	Scope of work.....	35

1.4.5 Plan of work	35
1.5 Format of the thesis.....	36
1.6 References.....	38

Chapter-2: Materials and experimental methods

2.1 Introduction.....	55
2.2 Raw materials.....	55
2.2.1 Polypropylene.....	56
2.2.2 Vamac Ultra IP.....	59
2.3 Gamma irradiation	64
2.4 Blend preparation.....	65
2.4.1 Twin screw extruder.....	65
2.4.2 Micro-compounder.....	66
2.5 Moulding of samples.....	67
2.5.1 Compression moulding	67
2.5.2 Microinjection moulding.....	68
2.6 Batch foaming.....	69
2.7 Characterizations techniques	70
2.7.1 Thermogravimetric analysis (TGA).....	70
2.7.2 Differential scanning calorimetry (DSC)	71
2.7.3 Scanning electron microscopy (SEM).....	73
2.7.3.1 <i>Secondary electron SEM</i>	73
2.7.3.2 <i>Backscattered electron SEM</i>	74
2.7.4 Parallel plate rheology.....	75

2.7.5 Dynamic mechanical analysis	76
2.7.6 1D wide angle x-ray analysis	77
2.7.7 Fourier transformed infra-red spectroscopy (FTIR).....	77
2.7.8 Nuclear magnetic resonance spectroscopy (NMR)	78
2.7.9 Gel content	79
2.7.10 Mechanical characteristics	79
2.7.10.1 Tensile test.....	80
2.7.10.2 Impact test	80
2.7.11 Contact angle measurement	81
2.7.12 Density measurement	81
2.8 References:.....	83

Chapter-3: PP/elastomer blends and optimization of foamability using design of experiment

3.1 Introduction.....	84
3.2 Materials and methods	85
3.2.1 Materials.....	86
3.2.2 Blend preparation	86
3.2.3 Foaming of blends	87
3.2.4 Foaming parameter optimization through design of experiment (DOE) approach.....	87
3.3 Blend morphology by SEM	92
3.4 X-ray diffraction characteristics of PP/elastomer blends.....	93
3.5 Rheological footprints of blends.....	95
3.6 Density and volume expansion ratio determination of foams and parametric optimization ..	97

3.7 Scanning electron microscopy of foams in optimization study	99
3.7.1 Parametric optimization based on cell size	101
3.7.2 Parametric optimization based on cell density	103
3.8 Summary	105
3.9 References	106

Chapter-4: Gamma irradiation of PP/elastomer blends and their characterizations

4.1 Introduction	108
4.2 Materials and methods	108
4.2.1 Materials	109
4.2.2 Blend preparation	109
4.2.3 Gamma irradiation of blends	109
4.2.4 Gel content determination of γ -irradiated samples of raw materials.....	109
4.3 Frequency sweep responses of pure polymers and blends.....	110
4.4 Fourier transformed infra-red (FTIR) spectroscopic characteristics	116
4.5 Melt and crystallization behaviour by differential scanning calorimetry (DSC).....	118
4.6 Thermogravimetric analysis (TGA) responses and degradation behaviour	122
4.7 Summary	129
4.8 References	130

Chapter-5: PP/gamma irradiated elastomer blends and their foamability

5.1 Introduction	131
5.2 Background of the present work	132

5.3 Materials and methods	133
5.3.1 Materials.....	134
5.3.2 Blend preparation	134
5.3.3 Foaming conditions of blends	136
5.4 Rheological study by slit capillary channel of micro-compounder during blend preparation	136
5.5 Blend morphology characterization	137
5.6 Rheological study by frequency sweep in a parallel plate instrument.....	138
5.7 Density measurement of foams.....	142
5.8 Foam morphology characterization	144
5.9 Effect of surface tension of neat polymers (from contact angle measurement)	151
5.10 Influence of morphology of blends on the nucleation and growth of cell	152
5.11 Summary.....	156
5.12 References.....	157

Chapter-6: Characterizations of PP/gamma irradiated elastomer blends

6.1 Introduction.....	159
6.2 Materials and methods	159
6.2.1 Materials.....	160
6.2.2 Blend preparation	160
6.3 Evaluation of blend morphology by SEM micrographs	163
6.4 Crystallizing behavior of blends using DSC.....	165
6.5 Dynamic-mechanical responses of blends	167
6.6 X-ray diffraction characteristics of blends.....	170

6.7 Rheological footprints of blends.....	171
6.8 Tensile behavior of blends.....	173
6.8.1 Tensile modulus.....	175
6.8.2 Tensile strength.....	177
6.8.3 Strain at break.....	181
6.9 Impact behaviour of blends.....	182
6.9.1 Impact strength.....	182
6.9.2 Evaluation of impact fracture behavioral change of blends by SEM micrographs of impact fractured surface.....	183
6.10 Summary.....	185
6.11 References.....	188

Chapter-7: Mechanical performance of foams of PP/gamma irradiated elastomer blends

7.1 Introduction.....	190
7.2 Materials and Methods.....	191
7.2.1 <i>Materials</i>	191
7.2.2 <i>Foaming of blends</i>	191
7.3 Density measurement of foams.....	192
7.4 Morphology characterization of foams by SEM.....	194
7.5 Tensile characteristics of foams.....	197
7.6 Thermal analysis of foams by DSC.....	202
7.7 WAXD analysis of foams.....	204
7.8 Impact properties of foams.....	206

7.9 Summary	208
7.10 References	210

Chapter-8: Summary, conclusion and future scope

8.1 Introduction.....	211
8.2 Summary	211
8.3 Conclusions.....	216
8.4 Future scope	217

LIST OF FIGURES

Chapter-1: Introduction and literature review

Figure 1.1 Surface indentation profiles upon adhesion. Coloured data show surface profiles of silicone substrates upon adhesion to spherical silica particles of radii 15 μm . No external forces are applied to the particles except for their weight, which causes negligible indentation. Substrate stiffnesses are 3 kPa (blue), 85 kPa (magenta) and 500 kPa (cyan) [1]..... 2

Figure 1.2 Plausible sites for cell nucleation (homogeneous or heterogeneous) in any foaming process of polymer blend..... 9

Figure 1.3 Schematic representation of batch foaming process..... 13

Figure 1.4 Variation of T_c as a function of the CO_2 pressure (p) for PET [88] 14

Figure 1.5 Depression of T_g , T_m and upper and lower limits for the foaming temperature and corresponding saturation pressure for PP [27]..... 18

Figure 1.6 Temperature range (ΔT) as a function of the saturation pressure for PP [27] 18

Figure 1.7 Gibb’s free energy of homogeneous and heterogeneous nucleation of a bubble 22

Figure 1.8 Schematic representation of foaming mechanism of PP/elastomer blend..... 27

Figure 1.9 Scheme of the study..... 34

Figure 1.10 Work plan describing the (a) Optimization of foaming parameters, characterizations of blends and foams, (b) Effects of extent of crosslinking on foaming..... 37

Chapter-2: Materials and experimental methods

Figure 2.1 TGA and DTGA thermograms of PP 57

Figure 2.2 DSC thermograms of PP..... 58

Figure 2.3 FTIR spectrum of PP 58

Figure 2.4 Characteristic XRD diffractogram of PP.....	59
Figure 2.5 TGA and DTGA thermograms of AEM.....	60
Figure 2.6 DSC thermograms of AEM	60
Figure 2.7 Characteristic FTIR spectrum of AEM	62
Figure 2.8 Characteristic ¹ H NMR spectrum of AEM.....	62
Figure 2.9 Characteristic ¹³ C NMR spectrum of AEM.....	63
Figure 2.10 Characteristic XRD diffractogram of AEM	63
Figure 2.11 Gamma radiation chamber (GC 1200, Board of Radiation and Isotope Technology, Department of Atomic Energy, India)	64
Figure 2.12 Twin screw extruder (OMega 20, STEER Engineering Pvt. Ltd., India).....	65
Figure 2.13 Micro compounder (Thermo Scientific, Haake MiniLab II, Germany).....	66
Figure 2.14 Compression moulding machine (Carver INC, USA).....	67
Figure 2.15 Micro injection molding machine (HAAKE Mini Jet II).....	68
Figure 2.16 Batch foaming set up	69
Figure 2.17 Thermo gravimetric analyzer (Perkin Elmer, Pyris 6)	71
Figure 2.18 Differential scanning calorimetry (TA instruments [DSC Q200]).....	72
Figure 2.19 Scanning electron microscope (ZEISS EVO 50)	73
Figure 2.20 Scanning electron microscope (FEI Quanta 200F).....	75
Figure 2.21 Parallel plate rheometer (Bohlin C-VOR instrument).....	76
Figure 2.22 Dynamic mechanical analyzer (TA instruments [DMA Q800])	76
Figure 2.23 X-Ray Diffractometer (Philips X'Pert Pro, PANalytical).....	77
Figure 2.24 Fourier transfer infrared spectrometer (Thermo Scientific NICOLET 6700)	78
Figure 2.25 Nuclear magnetic resonance spectrometer (Bruker DPX-400)	78
Figure 2.26 Tensile testing machine (Zwick Z/010).....	80

Figure 2.27 Notched impact tester (Tinius Olsen).....	80
Figure 2.28 Contact angle tester, DSA100 (Krüss, Germany).....	81

Chapter-3: PP/elastomer blends and optimization of foamability using DOE

Figure 3.1 (a) and (c) SEM micrograph of foam respectively at condition-1 and condition-2 of one of the three Taguchi confirmation experiments; whereas, (b) and (d) histogram obtained by the image analysis of SEM micrograph of one of the three Taguchi confirmation experiments at condition-1 and condition-2 respectively.....	92
Figure 3.2 Surface morphology of solvent etched blends (1.a) PPAEM-05, (2.a) PPAEM-10, (3.a) PPAEM-20 and (4.a) PPAEM-30 and histograms of particle sizes (1.b) PPAEM-05, (2.b) PPAEM-10, (3.b) PPAEM-20 and (4.b) PPAEM-30 respectively	94
Figure 3.3 (a) Wide angle X-ray (WAXD) diffractograms of two raw materials and their blends and (b) Percentage crystallinity change with composition	94
Figure 3.4 Rheological plots, (a) elastic modulus (G') vs. frequency, (b) tan delta ($\tan\delta$) vs. frequency, (c) Complex viscosity (η^*) vs. frequency and (d) van Grup-Palmen (vGP) plot of blends	95
Figure 3.5 (a) effect of control factors on volume expansion ratio (plot of S/N ratio) and (b) residual plots for volume expansion ratio	97
Figure 3.6 SEM micrographs (designated by (i)) and their histograms (designated by (ii)) of foam samples achieved in (1) observation -1, (2) observation -2 and (3) observation -3 of Run 9 respectively	100
Figure 3.7 (a) effect of control factors on cell size (plot of S/N ratio) and (b) residual plots for cell size.....	102
Figure 3.8 (a) effect of control factors on cell density (plot of S/N ratio) and (b) residual plots for cell density.....	104

Chapter-4: Gamma irradiation of PP/elastomer blends and their characterizations

- Figure 4.1** Elastic modulus vs. frequency plots of (a) PP, (b) PPAEM-05, (c) PPAEM-10, (d) PPAEM-20, (e) PPAEM-30 and (f) AEM irradiated at different γ -radiation doses (0, 12.5, 25, 50, 100 and 250 kGy)..... 112
- Figure 4.2** Complex viscosity vs. frequency plots of (a) PP, (b) PPAEM-05, (c) PPAEM-10, (d) PPAEM-20, (e) PPAEM-30 and (f) AEM irradiated at different γ -radiation doses (0, 12.5, 25, 50, 100 and 250 kGy)..... 114
- Figure 4.3** Tan delta vs. frequency plots of (a) PP, (b) PPAEM-05, (c) PPAEM-10, (d) PPAEM-20, (e) PPAEM-30 and (f) AEM irradiated at different γ -radiation doses (0, 12.5, 25, 50, 100 and 250 kGy) 115
- Figure 4.4** FTIR spectra of (a) PP and its γ -irradiated samples and (b) PP, AEM, PPAEM-30 and γ -irradiated samples of PPAEM-30 117
- Figure 4.5** 2nd heating endotherms of (a) PP, (b) PPAEM-05, (c) PPAEM-10, (d) PPAEM-20, (e) PPAEM-30 and (f) AEM at different γ -radiation doses (0, 12.5, 25, 50, 100 and 250 kGy)..... 118
- Figure 4.6** Changes in (a) Normalized percentage total crystallinity (χ), (b) melting point (T_m), (c) Full width at half maxima for fusion ($FWHM_m$) and (d) Glass transition temperature (T_g), derived from heating endotherms of PP, its blends (PPAEM-05, PPAEM-10, PPAEM-20 and PPAEM-30) and their γ -irradiated samples at different γ -radiation doses (0, 12.5, 25, 50, 100 and 250 kGy) 119
- Figure 4.7** (a) T_c and (b) $FWHM_c$ derived from the cooling thermograms of PP, its blends and their γ -radiated samples at different γ -radiation doses (0, 12.5, 25, 50, 100 and 250 kGy) 122
- Figure 4.8** (a) TGA and (b) DTGA thermograms or first derivatograms of PP exposed under different radiation doses and (c) TGA and (d) DTGA thermograms AEM irradiated at different γ -radiation doses (0, 12.5, 25, 50, 100 and 250 kGy) 123

Figure 4.9 Freeman-Carroll plots for the degradation of (a) PP and (b) AEM irradiated at different γ -radiation doses (0, 12.5, 25, 50, 100 and 250 kGy) 124

Chapter-5: PP/gamma irradiated elastomer blends and their foamability

Figure 5.1 (a) DMA storage modulus vs. temperature plot of PP and AEM; (b) Density vs. gamma irradiation dose of AEM, foamed at a temperature 80 °C, saturation pressure of 80 bar, saturation time of 1h and depressurization rate of 10 bar/s 132

Figure 5.2 Rheological plots (a) torque vs. time plot, and (b) viscosity vs. shear rate plot of different blends 136

Figure 5.3 SE SEM images of solvent etched morphology of (a.1) P-0AE/50, (a.2) P-0AE/100, and (a.3) P-0AE/200; and BSE SEM images of cryofractured morphology of (b.1) P-12.5AE/50, (b.2) P-12.5AE/100, (b.3) P-12.5AE/200, (c.1) P-25AE/50, (c.2) P-25AE/100, (c.3) P-25AE/200, (d.1) P-50AE/50, (d.2) P-50AE/100, and (d.3) P-50AE/200..... 139

Figure 5.4 Parallel plate rheological plots, (a) elastic modulus (G') versus angular frequency, (b) tan delta ($\tan\delta$) versus angular frequency, (c) complex viscosity (η^*) versus angular frequency, and (d) van Grunp–Palmen (vGP) plot of PP (-■-) and blends [P-0AE/200 (-●-), P-12.5AE/200 (-▲-), P-25AE/200 (-▼-), P-50AE/200 (-◆-)], obtained at 200 rpm screw speed 140

Figure 5.5 Effect of screw speed and extent of crosslinking on foam density of blends at foaming temperature (a) 140 °C, (b) 155 °C, and (c) 160 °C 142

Figure 5.6 SEM micrographs of (a) P/50, (b) P/100, and (c) P/200 foams obtained at 140 °C; whereas, (d) P/50, (e) P/100, and (f) P/200 foams obtained at 160 °C respectively..... 144

Figure 5.7 SEM micrographs of (a) P-0AE/50, (b) P-0AE/100, and (c) P-0AE/200 foams obtained at 140 °C; whereas, (d) P-0AE/50, (e) P-0AE/100, and (f) P-0AE/200 foams obtained at 155 °C; whereas, (g) P-0AE/50, (h) P-0AE/100, and (i) P-0AE/200 foams obtained at 160 °C respectively 145

Figure 5.8 SEM micrographs of (a) P-12.5AE/50, (b) P-12.5AE/100, and (c) P-12.5AE/200 foams obtained at 140 °C; whereas, (d) P-12.5AE/50, (e) P-12.5AE/100, and (f) P-12.5AE/200

foams obtained at 155 °C; whereas, (g) P-12.5AE/50, (h) P-12.5AE/100, and (i) P-12.5AE/200 foams obtained at 160 °C respectively 146

Figure 5.9 SEM micrographs of (a) P-50AE/50, (b) P-50AE/100, and (c) P-50AE/200 foams obtained at 140 °C; whereas, (d) P-50AE/50, (e) P-50AE/100, and (f) P-50AE/200 foams obtained at 155 °C; whereas, (g) P-50AE/50, (h) P-50AE/100, and (i) P-50AE/200 foams obtained at 160 °C respectively 150

Figure 5.10 BSE SEM micrographs of foams at 200 rpm with varying irradiation dose and foaming temperature 154

Figure 5.11 Schematic representation of the difference in foam processability for blends with uncrosslinked and crosslinked elastomers respectively 155

Chapter-6: Characterizations of PP/gamma irradiated elastomer blends

Figure 6.1 SEM images (corresponds to ‘i’) of RuO₄ stained surfaces of (a.i) R-PPAEM-05, (b.i) R-PPAEM-10, (c.i) R-PPAEM-20, (d.i) R-PPAEM-30; solvent etched surfaces (e.i) PPAEM-05, (f.i) PPAEM-10, (g.i) PPAEM-20 and (h.i) PPAEM-30 respectively and histograms (corresponds to ‘ii’) of (a.ii) R-PPAEM-05, (b.ii) R-PPAEM-10, (c.ii) R-PPAEM-20, (d.ii) R-PPAEM-30, (e.ii) PPAEM-05, (f.ii) PPAEM-10, (g.ii) PPAEM-20 and (h.ii) PPAEM-30 respectively 163

Figure 6.2 Schematic representation of final blend morphology development 164

Figure 6.3 DSC thermograms (a.i) 2nd heating endotherms, (a.ii) Cooling exotherms of PP/crosslinked AEM blends (PP, R-PPAEM-05, R-PPAEM-10, R-PPAEM-20 and R-PPAEM-30) and (b.i) 2nd heating endotherms, (b.ii) Cooling exotherms of PP/uncrosslinked AEM blends (PP, PPAEM-05, PPAEM-10, PPAEM-20 and PPAEM-30) 165

Figure 6.4 DMA plots (a.i) storage modulus (E'), (a.ii) loss modulus (E''), (a.iii) tan delta ($\tan\delta$) against temperature of PP/crosslinked AEM blends and (b.i) storage modulus (E'), (b.ii) loss modulus (E''), (b.iii) tan delta ($\tan\delta$) against temperature PP/uncrosslinked AEM blends 169

Figure 6.5 Wide angle X-ray diffractograms of (a) PP/ γ -irradiated elastomer blends and (b) PP/unirradiated elastomer blends 170

Figure 6.6 Rheological plots, (a.i) elastic modulus (G') vs. frequency, (b.i) tan delta ($\tan\delta$) vs. frequency, (c.i) complex viscosity (η^*) vs. frequency and (d.i) van Grup-Palmen (vGP) plot of PP/crosslinked AEM blends; whereas, (a.ii) elastic modulus (G') vs. frequency, (b.ii) tan delta ($\tan\delta$) vs. frequency, (c.ii) complex viscosity (η^*) vs. frequency and (d.ii) van Grup-Palmen (vGP) plot of PP/uncrosslinked AEM blends respectively.....	172
Figure 6.7 Stress-strain plots of (a) Crosslinked AEM elastomer, (b) Uncrosslinked AEM elastomer, (c) PP/crosslinked AEM blends and (d) PP/uncrosslinked AEM blends.....	174
Figure 6.8 Relative tensile modulus (E_b/E_m) vs. ϕ_r plots and comparison with predictive models for (a) PP/crosslinked AEM blends and (b) PP/uncrosslinked AEM blends.....	176
Figure 6.9 Theoretical models (a) Neilsen's first power-law model, (b) Nicolais-Narkis model and (c) porosity model, fitted against the experimental relative tensile strength (I_b/I_m) vs. ϕ_r plots for PP/crosslinked AEM blends.....	178
Figure 6.10 Theoretical models (a) Neilsen's first power-law model, (b) Nicolais-Narkis model and (c) porosity model, fitted against the experimental relative tensile strength (I_b/I_m) vs. ϕ_r plots for PP/uncrosslinked AEM blends.....	180
Figure 6.11 Relative strain at break (ϵ_b/ϵ_m) vs. ϕ_r plots of PP/crosslinked AEM blends and PP/uncrosslinked AEM blends	181
Figure 6.12 Relative impact strength (I_b/I_m) vs. ϕ_r plots of PP/crosslinked AEM blends and PP/uncrosslinked AEM blends	182
Figure 6.13 SEM micrographs of impact fractured surfaces of (a.i) R-PPAEM-05, (b.i) PPAEM-05, (a.ii) R-PPAEM-10, (b.ii) PPAEM-10, (a.iii) R-PPAEM-20, (b.iii) PPAEM-20, (a.iv) R-PPAEM-30 and (b.iv) PPAEM-30.....	184

Chapter-7: Mechanical performance of foams of PP/gamma irradiated elastomer blends

Figure 7.1 SEM micrographs of foams of (a) PP, (b) R-PPAEM-05, (c) R-PPAEM-10, (d) R-PPAEM-20, (e) R-PPAEM-30, (f) PPAEM-05, (g) PPAEM-10, (h) PPAEM-20, and (i) PPAEM-30 obtained at OC-1	195
---	-----

Figure 7.2 SEM micrographs of foams of (a) PP, (b) R-PPAEM-05, (c) R-PPAEM-10, (d) R-PPAEM-20, (e) R-PPAEM-30, (f) PPAEM-05, (g) PPAEM-10, (h) PPAEM-20, and (i) PPAEM-30 obtained at OC-2	195
Figure 7.3 SEM micrographs of foams of (a) PP, (b) R-PPAEM-05, (c) R-PPAEM-10, (d) R-PPAEM-20, (e) R-PPAEM-30, (f) PPAEM-05, (g) PPAEM-10, (h) PPAEM-20, and (i) PPAEM-30 obtained at OC-3	196
Figure 7.4 Stress-strain plots of foams at (a) OC-1, (b) OC-2, and (c) OC-3.....	198
Figure 7.5 (a) Tensile strength, (b) Tensile modulus, (c) Specific tensile strength, and (d) Specific tensile modulus, and (e) Strain at break of neat and foams of PP and blends	200
Figure 7.6 Application of Gibson and Ashby model on foams of blends.....	201
Figure 7.7 DSC thermograms of (a) PP, (b) R-PPAEM-10 and (c) PPAEM-10 foams	203
Figure 7.8 WAXD diffractograms of unfoamed and foam samples of (a) PP, (b) R-PPAEM-10 and (c) PPAEM-10, foamed at three conditions, such as, OC-1, OC-2 and OC-3	205
Figure 7.9 (a) Impact strength, and (b) Specific impact strength of neat and foams of PP and blends	206
Figure 7.10 SEM micrographs of impact fractured surfaces of foams of (a) PP, (b) R-PPAEM-10, (c) R-PPAEM-30, (d) PPAEM-10 and (e) PPAEM-30, foamed at three different foaming conditions OC-1 (designated by 1), OC-2 (designated by 2) and OC-3 (designated by 3) respectively	207

LIST OF TABLES

Chapter-2: Materials and experimental methods

Table 2.1 Raw Materials; its Grades, Supplier and Characteristics	55
Table 2.2 Characteristics of PP (Propel 1030FG)	56
Table 2.3 Characteristics of AEM.....	61

Chapter-3: PP/elastomer blends and optimization of foamability using DOE

Table 3.1 Details of compositions and their properties.....	86
Table 3.2 Parameters of design and levels of various control factors.....	87
Table 3.3 L_{16} ($4^4 2^2$) orthogonal array.....	89
Table 3.4 ANOVA table for volume expansion ratio	98
Table 3.5 Results of the confirmation experiment at condition-1 and condition-2.....	99
Table 3.6 SEM morphological data of Run – 9.....	100
Table 3.7 ANOVA table for cell size.....	102
Table 3.8 ANOVA table for cell density.....	104

Chapter-4: Gamma irradiation of PP/elastomer blends and their characterizations

Table 4.1 Gel content of raw materials at different γ -radiation doses	110
Table 4.2 Parameters obtained from TGA, DTGA thermograms and Freeman-Carroll technique for PP irradiated at different γ -radiation doses	126

Table 4.3 Parameters obtained from TGA, DTGA thermograms and Freeman-Carroll technique for PPAEM-05, PPAEM-10, PPAEM-20, PPAEM-30 and AEM irradiated at different γ -radiation doses	127
--	-----

Chapter-5: PP/gamma irradiated elastomer blends and their foamability

Table 5.1 Details of compositions and sample designations.....	134
Table 5.2 Particle sizes of AEM elastomers in blends at different extent of crosslinking and different speed of mixing	138
Table 5.3 Effect of foaming temperature, and screw speed (during blend morphology development) on cell size, and cell density of PP and its blends.....	148
Table 5.4 Contact angle and surface tension of PP, AEM and R-AEM	152

Chapter-6: Characterizations of PP/gamma irradiated elastomer blends

Table 6.1 Details of compositions and their properties.....	161
Table 6.2 Tensile test results, theoretical model parameters and impact test results of PP/crosslinked AEM blends and PP/uncrosslinked AEM blends.....	175

Chapter-7: Mechanical performance of foams of PP/gamma irradiated elastomer blends

Table 7.1 Characteristics (cell size, cell density and density) of foams.....	193
Table 7.2 DSC data of neat and foamed samples.....	202

LIST OF EQUATIONS

1.1	Gibb's free energy for homogeneous nucleation.....	23
1.2	Gibb's free energy for heterogeneous nucleation.....	23
2.1	Freeman-Carroll single heating rate equation.....	71
2.2	Normalized percentage total crystallinity.....	72
2.3	Number average cell size of foam.....	74
2.4	Cell density of foam.....	74
2.5	Percentage gel content of crosslinked sample.....	79
2.6	Density of sample.....	82
2.7	Volume expansion ratio of sample.....	82
3.1	Signal to noise ratio for "smaller is better" characteristics.....	90
3.2	Signal to noise ratio for "bigger is better" characteristics.....	90
3.3	Basic predicted average of signal to noise ratio.....	91
3.4	Final predicted average of signal to noise ratio.....	91
4.1	Rule of mixture for the thermal stability of blends.....	126
5.1	Equation of correlation between surface tension and contact angle for water.....	151
5.2	Equation of correlation between surface tension and contact angle for Polyethylene glycol 200.....	151
5.3	Equation of interfacial tension.....	152
6.1	Rule of mixture of tensile modulus.....	176
6.2	Foam model for tensile modulus.....	176
6.3	Neilsen's first power-law model for tensile strength.....	177
6.4	Nicolais-Narkis model for tensile strength.....	177
6.5	Porosity model for tensile strength.....	177
7.1	Gibson and Ashby model.....	201

LIST OF ABBREVIATIONS

Abbreviation	Description
AEM	: Ethylene acrylic elastomer
ANOVA	: Analysis of variance
BSE	: Backscattered electron
CBA	: Chemical blowing agent
CD	: Cell density
CFC	: Chlorofluorocarbon
CS	: Cell size
DCP	: Dicumyl peroxide
DF	: Degrees of freedom
DMA	: Dynamic mechanical analysis
DOE	: Design of experiment
DSC	: Differential scanning calorimetry
DTGA	: Differential thermogravimetric analysis
E-b-P	: Ethylene propylene block copolymer
EMA	: Ethylene methyl acrylate elastomer
EOC	: Ethylene octane copolymer
EPDM	: Ethylene propylene di-ene rubber
EPE	: Expanded polyethylene
EPP	: Expanded polypropylene
EPR	: Ethylene propylene rubber
EPS	: Expanded polystyrene
E-r-P	: Ethylene propylene random copolymer
EVA	: Ethylene vinyl acetate
FTIR	: Fourier transformed infra-red spectroscopy
$FWHM_c$: Full width at half maxima for crystallization
$FWHM_m$: Full width at half maxima for fusion

HCFC	:	Hydrochlorofluorocarbon
HDPE	:	High density polyethylene
HFC	:	Hydrofluorocarbon
HMSPP	:	High melt strength polypropylene
IPD	:	Interparticle distance
iPP	:	Isotactic polypropylene
LDPE	:	Low density polyethylene
LLDPE	:	Linear low density polyethylene
MFI	:	Melt flow index
NG	:	No gel
NMR	:	Nuclear magnetic resonance spectroscopy
OA	:	Orthogonal array
PBA	:	Physical blowing agent
PE	:	Polyethylene
PEG200	:	Polyethylene glycol 200
PET	:	Polyethylene terephthalate
POE	:	Polyethylene-octene elastomer
PP	:	Polypropylene
SBS	:	Styrene butadiene styrene rubber
scCO ₂	:	Supercritical carbon dioxide
SE	:	Secondary electron
SEM	:	Scanning electron microscope
SS	:	Sum of squares
TAIC	:	Triallylisocyanurate
TGA	:	Thermogravimetric analysis
TPO	:	Thermoplastic olefin
TPS	:	Thermoplastic polystyrene elastomer
TPV	:	Thermoplastic vulcanizate
TSE	:	Twin screw extruder
UF	:	Unfoamed material
UHMWPE	:	Ultra high molecular weight polyethylene

UTM	:	Universal testing machine
V.R.	:	Viscosity ratio
VER	:	Volume expansion ratio
vGP plot	:	van Grup-Palmen plot
WAXD	:	Wide angle X-ray diffraction
WGRT	:	Waste ground rubber tire
XRD	:	X-ray diffraction

LIST OF SYMBOLS

Symbol	Description
2θ	: X-ray scattering angle
A	: Area of the SEM micrograph (centimeters squared)
C	: Gibson and Ashby parameter
d	: Number average cell size
D_n	: Number average particle size
D_w	: Weight average particle size
E	: Tensile modulus / Tensile moduli of foam
E'	: Storage modulus
E''	: Loss modulus
E_0	: Tensile moduli of non-porous material
E_a	: Activation energy for degradation
$E_{a(m)}$: Activation energy of matrix
$E_{a(r)}$: Activation energy of elastomer
$E_{a(theo)}$: Activation energy of blend evaluated theoretically
E_b	: Tensile modulus of blend
E_b/E_m	: Relative tensile moduli
E_d	: Tensile modulus of elastomer
E_m	: Tensile modulus of matrix
F	: Corrected factor of heterogeneous nucleation/ geometrical factor
G^*	: Complex modulus
G'	: Elastic modulus
G''	: Viscous modulus
I	: Impact strength
I_b	: Impact strength of blend
I_b/I_m	: Relative impact strength
I_m	: Impact strength of matrix
K_b	: Interphase interaction parameter in Nicolais-Narkis model

m_1	:	Weight of sample in air
m_2	:	Weight of sample along with sinker in fluid
m_s	:	Weight of sinker in fluid
n	:	Order of degradation
n	:	Gibson and Ashby parameter
N_c	:	Cell density
R	:	Universal gas constant
R^2	:	Coefficient of determination
S	:	Neilsen parameters for first power-law model
S/N	:	Signal to noise ratio
T	:	Absolute temperature
$\tan\delta$:	Tan delta
T_c	:	Crystallization temperature
T_g	:	Glass transition temperature
T_i	:	Initiation degradation temperature
T_m	:	Melting temperature
T_m	:	Maximum degradation temperature
W_{el}	:	Weight fraction of elastomer present in blends
W_f	:	Final weight of sample
W_{het}	:	Free energy barrier for initiating the heterogeneous nucleation
W_{het}	:	Surface geometries of the nucleating agents
W_i	:	Initial weight of sample
wt. %	:	Weight percentage
A	:	Degree of conversion at time t
α	:	Porosity model parameter
γ	:	Surface tension
γ_{12}	:	Interfacial tension between materials 1 and 2
γ^d	:	Dispersive component of the surface tension
γ^p	:	Polar component of the surface tension
γ -radiation	:	Gamma radiation

δ	:	Phase angle
ΔH_c	:	Enthalpy of melting
$\Delta H_{experimental}$:	Experimentally achieved enthalpy of fusion of PP
$\Delta H_{theoretical}$:	Theoretically determined enthalpy of fusion of 100% crystalline PP
ΔP	:	Pressure exerted by the scCO ₂ on the cell walls
ΔT	:	Temperature range
ε	:	Strain at break
ε_b	:	Strain at break of blend
$\varepsilon_b/\varepsilon_m$:	Relative strains at break
ε_m	:	Strain at break of matrix
η^*	:	Complex viscosity
θ / θ_c	:	Contact angle
ρ	:	Density
ρ	:	Density/ Density of foam
ρ_f	:	Density of the foamed sample
ρ_{fl}	:	Specific gravity of the fluid
ρ_o	:	Density of non-porous material
ρ_u	:	Density of the unfoamed sample
σ	:	Tensile strength
σ_b	:	Tensile strength of blend
σ_b/σ_m	:	Relative tensile strength
σ_m	:	Tensile strength of matrix
τ	:	Shear stress
φ	:	Volume expansion ratio
φ_r	:	Volume fraction
χ	:	Crystallinity percentage/Total crystallinity percentage
ω	:	Frequency
ΔG_{homo}^*	:	Gibb's free energy for homogeneous nucleation
ΔG_{het}^*	:	Gibb's free energy for heterogeneous nucleation
\bar{d}	:	Average cell size of foam
\bar{N}_c	:	Average cell density of foams

$\bar{\eta}$:	Predicted average of signal to noise ratio
\bar{T}	:	Overall experimental average of signal to noise ratio
$\dot{\gamma}$:	Shear rate